EPJ Web of Conferences **142**, 01004 (2017) DOI: 10.1051/epjconf/201714201004
Advances in Dark Matter and Particle Physics

Overview of ALICE results on hadronic resonance production

Angela Badalà[1,a] for the ALICE Collaboration

[1] *INFN - Sezione di Catania , Via S. Sofia 64, 95123, Catania (Italy)*

Abstract. The measurement of hadronic resonance production in heavy-ion collisions is a valuable tool to study the properties of the hadronic phase. In addition, these measurements contribute to the study of particle production mechanisms, such as recombination and statistical hadronization, and can give information on the parton energy loss in the hot QCD medium. Measurement of a wide set of resonances with different lifetimes is useful to better characterize the hadronic phase and the time span between chemical and thermal freeze-out. Proton-proton (pp) collisions have been used extensively as a reference for the study of larger colliding systems, but recent measurements performed in high-multiplicity pp and proton-lead (p–Pb) collisions at the LHC have shown features that are reminiscent of those observed in lead-lead (Pb–Pb) collisions. Resonance measurements in small systems serve as a reference for heavy-ion collisions and contribute to searches for collective effects. An overview of recent results on hadronic resonance production measured in ALICE will be presented. Transverse momentum ($p_{\rm T}$) spectra, ratios of yield to that of long-lived hadrons of the $\rm K^*(892)^0$ and $\phi(1020)$ mesons in pp, p–Pb, and Pb–Pb collisions at LHC energies will be discussed. The most recent results include the measurement of resonance production in pp collisions at 7 TeV as a function of the charged-particle multiplicity, that will be compared to the results for other light hadrons as pions, kaons, protons, $\rm K^0_S$, Λ, Ξ^-, Ω^-. In addition, the $p_{\rm T}$ spectra and yields of the $\rho(770)^0$ meson in pp and Pb–Pb collisions at $\sqrt{s_{\rm NN}}$ = 2.76 TeV and of $\Sigma(1385)^{\pm}$ and $\Xi(1530)^0$ baryons in p–Pb collisions at $\sqrt{s_{\rm NN}}$ = 5.02 TeV will be presented.

1 Introduction

Hadronic resonances, along with stable hadrons, allow the study of properties of heavy-ion collisions, both in the early (quark-gluon plasma) and late (hadronic) stage of their evolution. Modification of their yield after chemical freeze-out is expected due to the regeneration and re-scattering effects in the hadronic phase, which are expected to have their greatest strength at low transverse momentum. Final resonance yields depend on the scattering cross sections of their decay products and the timescale between the chemical and the kinetic freeze-out compared to the resonance lifetime, which determine the fraction of 'undetected' particles. However resonances may be regenerated by pseudo-elastic interactions in the hadronic medium. Therefore, resonances with different lifetimes are good candidates to probe the interplay of particle re-scattering and regeneration in the hadronic phase. Comparison of such measurements to theoretical models [1, 2] allows for an estimation of the timescale between chemical and kinetic freeeze-out.

Measurements of resonance and stable-hadron yields may be used to estimate properties of the hadronic phase of heavy-ion collisions, such as temperature and lifetime. Information on the particle production mechanisms can be derived from the comparison of particles with similar mass but different baryon number and/or strangeness content. Then comparison of resonance production with that of long lived hadrons can be interesting in this respect. In particular, for strangeness production it is worth studying the ϕ meson with its hidden strangeness content.

Both meson and baryon resonances have been measured by the ALICE experiment [3] in different collisions systems (pp, p–Pb, Pb–Pb) at LHC energies [4–8]. Resonance measurements in pp and p–Pb systems are useful as references and may help in disentangling initial-state effects from genuine in-medium effects, which may occur in Pb–Pb collisions. At LHC in p–Pb collisions final state dense matter effects could be present considering that the pseudo-rapidity density of final state particles reaches value similar to central collisions at top RHIC energy [9]. Moreover parton shadowing and/or novel phenomena like saturation as implemented in the Color Glass Condensate model [10] may become apparent due to the low fractional parton momentum x and the high gluon density reached in the initial state. Deconfinement and collectivity effects are not expected in pp collisions and for this reason they have been often used as reference for larger systems. Recently, in high-multiplicity pp and p–Pb collisions LHC experiments have observed features tradionally associated to the formation of a strongly-interacting quark-gluon medium and hinting at the presence of collective phenomena [11–13]. This has triggered the investigation of collectivity-driven features in small systems and the study of strangeness production as a function of the multiplicity in p–Pb and pp collisions [14–17].

[a] e-mail: Angela.Badala@ct.infn.it

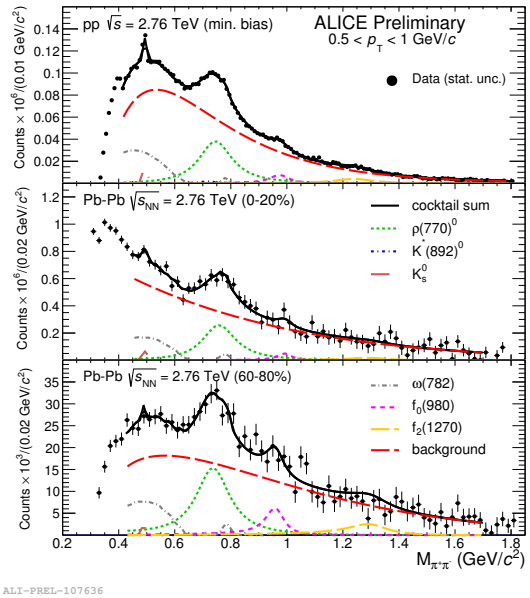

Figure 1. (color online) Invariant mass distributions for π^++π^- pairs with p_T in the range 0.5-1.0 GeV/c in minimum bias pp collisions at $\sqrt{s}$ = 2.76 TeV (upper panel) and in Pb–Pb collisions at $\sqrt{s_{NN}}$ = 2.76 TeV in the centrality range 0-20% (middle panel) and 60-80% (lower panel).

2 Resonance identification in ALICE

In pp and in Pb–Pb collisions resonances are measured in one unit of rapidity $|y| < 0.5$ in the centre-of-mass reference frame, while in p–Pb the rapidity range is restricted to -0.5 < y < 0, in order to ensure the best detector acceptance with the shifted centre-of-mass of the system. The position of the primary vertex is estimated using the tracks reconstructed in the Inner Tracking System (ITS) and in the Time Projection Chamber (TPC) and its component along the beam axis is required to be within 10 cm from the centre of the ALICE detector. A detailed review of the ALICE detector and its particle identification capabilities can be found in [3, 18]. The V0A and V0C detectors, two forward-rapidity scintillator hodoscopes, were used for event triggering and beam-gas rejection. To avoid autocorrelation bias the event class selection is based on the total charge deposited in the V0A and V0C detectors and for each event class the value of $\langle dN_{ch}/d\eta \rangle$ is estimated as the average number of primary charged tracks at mid-rapidity.

The $\rho(770)^0$, $K^*(892)^0$ and $\phi(1020)$ mesons (hereafter referred to as ρ^0, K^{*0}, ϕ) and the $\Sigma(1385)^{\pm}$ and $\Xi(1530)^0$ baryons (hereafter referred to as $\Sigma^{*\pm}$ and Ξ^{*0}) and their anti-particles are reconstructed by the invariant mass spectrum of their hadronic decays products ($\rho^0 \longrightarrow \pi^+ \pi^-$, $K^{*0} \longrightarrow \pi^{\pm} K^{\pm}$, $\phi \longrightarrow K^+K^-$, $\Sigma^{*\pm} \longrightarrow \Lambda\pi^{\pm}$, and $\Xi^{*0} \longrightarrow \Xi^-\pi^+$). Identification of pions and kaons is carried out using the measurement of the specific energy loss (dE/dx) in the TPC. The TPC dE/dx measurement allows pions to be separated from kaons for momenta up to $p \sim 0.7$ GeV/c, while the proton/antiproton band starts to overlap with the pion/kaon band at $p \sim 1$ GeV/c. An improvement in the significance of the signal has been achieved using the information from the Time-Of-Flight (TOF) detector for tracks for which it is available. The TOF allows pions and kaons to be unambiguously identified up to $p \sim$ 1.5-2.0 GeV/c. The two mesons can be distinguished from (anti)protons up to $p \sim 2.5$ GeV/c. For the baryonic resonances, the intermediate decay daughters Λ and Ξ^- are identified through selection based on their decay topologies.

Combinatorial backgrounds are estimated using either like-charge pairs or event mixing. They are subtracted from the distribution of the unlike-charge pairs for the different p_T and centrality/multiplicity intervals. The resulting invariant mass distributions are then fitted with a relativistic Breit-Wigner (K^{*0}, $\Sigma^{*\pm}$) or a Voigtian (ϕ, Ξ^{*0}) function added to a first or second order polynomial to describe the residual background (see [4–8] for further details). The background-subtracted invariant mass distributions obtained for π^++π^- pairs with p_T in the range 0.5-1.0 GeV/c in minimum bias pp collisions at $\sqrt{s}$ =2.76 TeV and in Pb–Pb collisions at $\sqrt{s_{NN}}$ = 2.76 TeV in the centrality range 0-20% and 60-80% are shown in the three panels of Fig. 1. The black curves in this figure represent the fit result. The fit function is given by a cocktail including a smooth function to describe a continuum residual background (dashed red curves in Fig. 1) plus peaks accounting for the contribution of the K^0_S, K^{*0}, 2- and 3-body decay of $\omega(782)$, $f_0(980)$ and $f_2(1270)$. The shape of the ρ^0 peak is described by the product of a relativistic p-wave Breit-Wigner function, a phase-space factor, a mass-dependent reconstruction efficiency, and a Söding interference term [19].

3 Resonance results in pp, p–Pb and Pb–Pb collisions

The procedure used to estimate the resonanance p_T spectrum has been extensively explained in [4–8]. To extract the particle yields and the $\langle p_T \rangle$, the spectra are fitted using a Lévy-Tsallis parameterization [20] (for pp and p–Pb collisions) or Boltzmann-Gibbs blast-wave functions [21] (for Pb–Pb collisions). To extract the dN/dy and the $\langle p_T \rangle$ the measured p_T distributions are integrated, while the fits are used to estimate the resonance yield at low and high p_T, where no signal could be measured. It may be noted that the extrapolated fraction of the total yield for the K^{*0} is lower than 0.1%.

The p_T spectra and the yields of the K^{*0} and ϕ have been measured in pp, p–Pb and Pb–Pb collisions at the various energies studied at LHC both in inclusive and in different multiplicity or centrality intervals. Similar information has been obtained for the ρ^0 in pp and Pb–Pb collisions at $\sqrt{s_{NN}}$ = 2.76 TeV and for the $\Sigma^{*\pm}$ and Ξ^{*0} in pp collisions at $\sqrt{s}$ = 7 TeV and in p–Pb collisions at $\sqrt{s_{NN}}$ = 5.02 TeV.

Using Run 2 data the K^{*0} and ϕ p_T spectra have been measured in inelastic pp collisions at $\sqrt{s}$ = 13 TeV. The

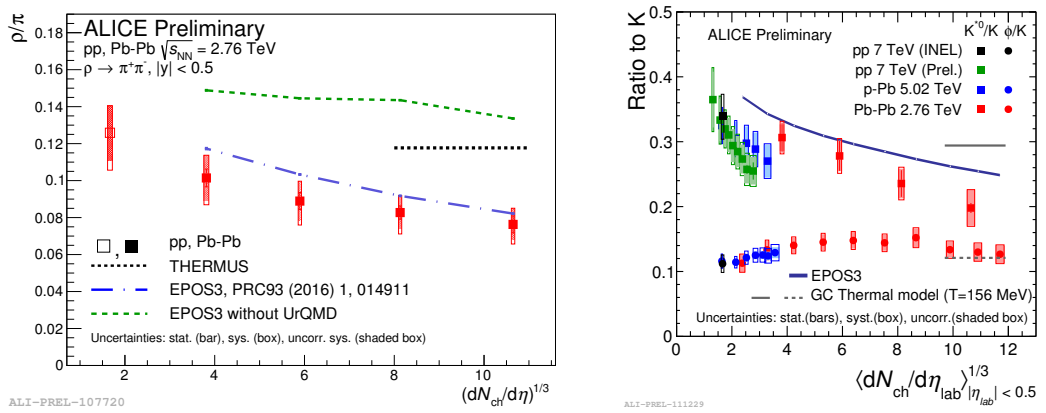

Figure 2. Ratios $\rho^0/\langle\pi^\pm\rangle$ (left panel), K^{*0}/K and ϕ/K (right panel) as a function of the cubic root of the charged particle multiplicity density $dN_{ch}/d\eta$ for various collision systems. For central collisions the values predicted by a grand-canonical thermal model are also shown [23]. The behaviour estimated by EPOS model [2] for K^{*0}/K ratio (continuous blue line) and $\rho^0/\langle\pi^\pm\rangle$ ratio (dashed blue line) are shown. The green dashed line in left panel represents the values of the $\rho^0/\langle\pi^\pm\rangle$ ratio estimated by EPOS if no final state interaction are taken into account.

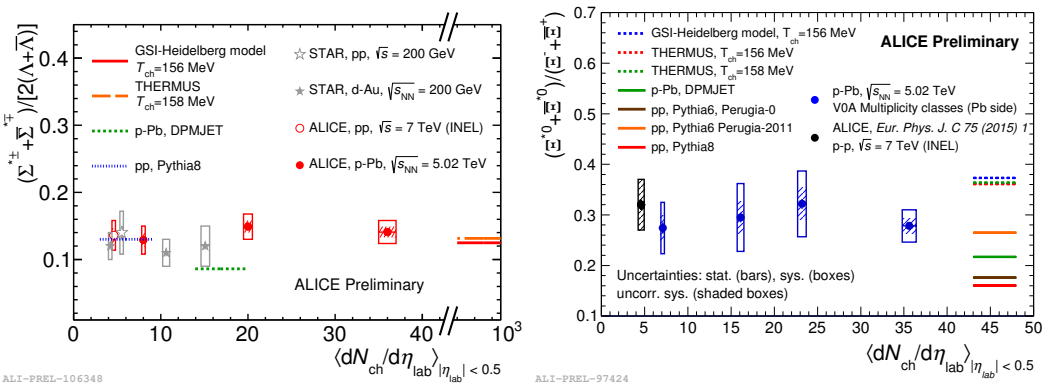

Figure 3. Ratios $(\Sigma^{*\pm}+\overline{\Sigma}^{*\mp})/2(\Lambda+\overline{\Lambda})$ (left panel) and $(\Xi^{*0}+\overline{\Xi}^{*0})/(\Xi^-+\overline{\Xi}^+)$ (right panel) measured in pp [8, 37], d–Au [38] and p–Pb collisions as a function of average charged particle density measured at mid-rapidity. Statistical uncertainties (bars) are shown together with total systematic uncertainties (hollow boxes) and systematic uncertainties uncorrelated across multiplicity (shaded boxes). Some model predictions are also shown [24–27] as lines at their appropriate abscissa, respectively.

comparison of the p_T-integrated K^{*0}/K and ϕ/K ratios obtained at this energy with the existing data show no energy dependence through 2-3 orders of magnitude in the collision energy.

In order to check the presence of a suppression in the production of the resonances and to study whether the strength of the suppression is related to the system size, the ratios of the p_T-integrated particle yields $\rho^0/\langle\pi^\pm\rangle$, K^{*0}/K and ϕ/K have been reported as a function of the cubic root of the charged particle multiplicity density $\langle dN_{ch}/d\eta\rangle^{1/3}$, for pp, p–Pb and Pb–Pb collisions, respectively, at $\sqrt{s}$ = 7 TeV and $\sqrt{s_{NN}}$ = 5.02 and 2.76 TeV (Fig. 2). A centrality-dependent suppression is clearly observed for $\rho^0/\langle\pi^\pm\rangle$ and K^{*0}/K in Pb–Pb collisions. In particular in central collisions the measured ratios are about 60% of the estimate of a grand-canonical thermal model [23], which does not include re-scattering effects. The observed suppression may be related to the pion rescattering mechanism $\sigma(\pi,\pi)$, which destroys the pion-pion and pion-kaon correlations. It is interesting to note that the behaviour of the ratios is at least qualitatively reproduced by calculations using the EPOS model [2], which takes the regeneration and rescattering effects of the resonance decay particles in the hadronic phase explicitly into account by UrQMD [22] (see blue curves in left and right panels of Fig. 2). On the contrary the ϕ, which lives 10 times longer than the K^{*0} and 35 times longer than the ρ^0, decays predominantly after the end of the hadronic phase and its yield should not be affected by regeneration and re-scattering effects. This seems to be

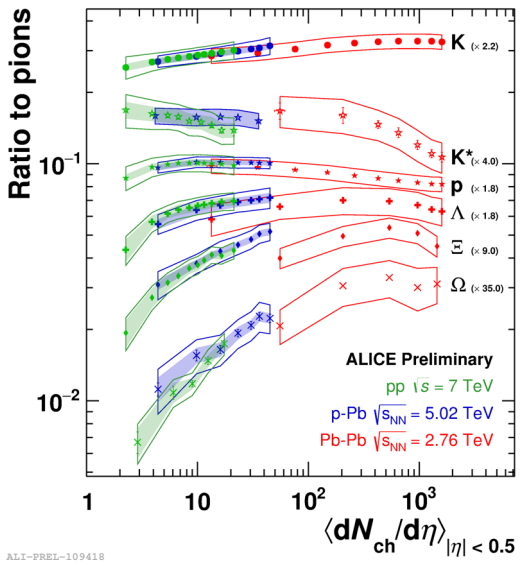

Figure 4. (color online) p_T-integrated yield ratios of K, K^{*0}, p, Λ, Ξ^-, Ω^- to pion as a function of average charged particle multiplicity at mid-rapidity in different collision systems: pp collisions at $\sqrt{s}$ = 7 TeV [17] (green symbols), p–Pb collisions [14, 15] at $\sqrt{s_{NN}}$ = 5.02 TeV (blue symbols) and Pb–Pb at $\sqrt{s_{NN}}$ = 2.76 TeV [33, 34] (red symbols). The hollow bands indicate the total systematic uncertainties, while the shaded ones represent the systematic uncertainties uncorrelated across multiplicity. These are shown only for pp and p–Pb collisions.

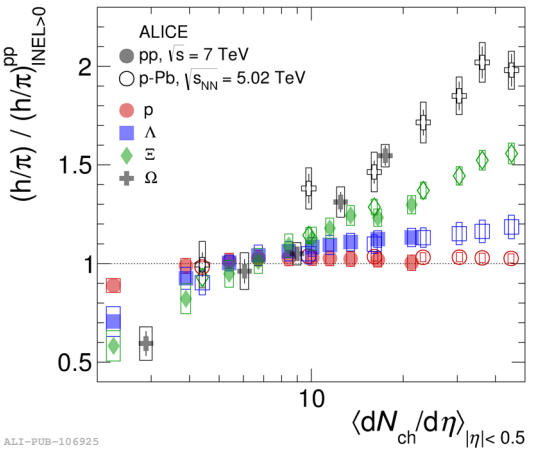

Figure 5. (color online) Particle yield ratios to pions of strange and multi-strange baryons and protons normalised to the values measured in the inclusive INEL>0 pp sample as a function of the average charged particle multiplicity, for pp at $\sqrt{s}$ = 7 TeV [17] and p–Pb at $\sqrt{s_{NN}}$ = 5.02 TeV [14, 15].

confirmed by the ϕ/K behavior. In fact it is rather independent of the event multiplicity class and in Pb–Pb collisions the distribution is almost flat and it is consistent with the estimate of a grand-canonical thermal model [23]. Furthermore, an apparent multiplicity-dependent suppression of the K^{*0}/K ratio has been observed in pp and p–Pb collisions, which may be an indication of the presence of a hadron-gas phase in high-multiplicity pp and p–Pb collisions.

In Fig. 3 the integrated particle ratios of excited hyperon to stable one as $(\Sigma^{*\pm}+\overline{\Sigma}^{*\mp})/2(\Lambda+\overline{\Lambda})$ (left panel) and $(\Xi^{*0}+\overline{\Xi}^{*0})/(\Xi^-+\overline{\Xi}^+)$ (right panel) measured in pp at $\sqrt{s}$ = 7 TeV [8] and p–Pb at $\sqrt{s_{NN}}$ = 5.02 TeV collisions are reported as a function of the average charged particle density and compared to results obtained from STAR in pp and d–Au collisions at $\sqrt{s_{NN}}$ = 200 GeV [38]. No multiplicity dependence is observed for these ratios in p–Pb collisions and they are consistent with the values measured in pp and d–Au collisions. The observed constant behaviour of the yield ratios of excited to ground-state hyperons with same strangeness content may indicate that neither regeneration nor re-scattering dominates with increasing collision system size, even for $\Sigma^{*\pm}$, which has a shorter lifetime than Ξ^{*0} by a factor of 4. Furthermore the constant behaviour of $\Sigma^{*\pm}/\Lambda$ ratio is in contrast with the apparent decrease observed for the K^{*0}/K ratio in a similar multiplicity range, considering the similarly short lifetimes of $\Sigma^{*\pm}$ and K^{*0}.

While the $\Sigma^{*\pm}/\Lambda$ ratios are consistent with PYTHIA8 [24] and thermal model predictions [26, 27] in pp and in p–Pb collisions, DPMJET [25] underpredicts the ratios obtained in p–Pb collisions. The same models are not able to estimate the Ξ^{*0}/Ξ^-values both in pp and in p–Pb collisions. In particular, PYTHIA8 [24] and DPMJET [25] estimates are lower while thermal model predictions [26, 27] are higher. For small systems a canonical treatment is a priori required to take into account exact strangeness conservation. However, for the chosen ratios the canonical corrections are identical for numerator and denominator, due to the same strangeness quantum number. Therefore, the grand canonical values can be used.

4 Strangeness production in pp, p–Pb and Pb–Pb

Strangeness enhancement was one of the first proposed QGP signatures [28]. At LHC (as SPS [29–31] and RHIC [32] energies) a clear increase of strangeness production from pp to Pb-Pb was observed [33, 34]. This strangeness enhancement is expected to be more pronounced for multi-strange baryons, and this was indeed observed in collisions of heavy nuclei. The abundances of strange particles in heavy-ion collisions are compatible with those of a hadron gas in thermal and chemical equilibrium and can be described using a grand canonical statistical model [23, 26]. The p–Pb results [14, 15] as a function of the average charged particle multiplicity density at mid-rapidity are consistent with pp results at low multiplicity and with central values of Pb–Pb collisions at high multiplicity.

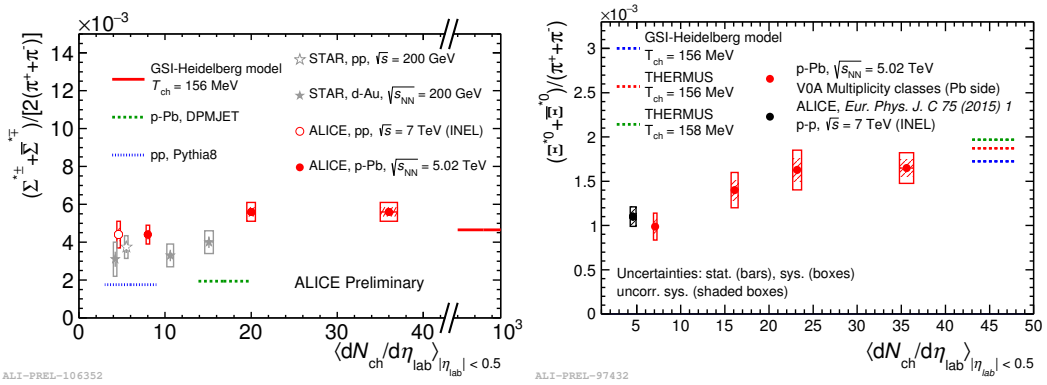

Figure 6. Ratios $(\Sigma^{*\pm}+\overline{\Sigma}^{*\mp})/2(\pi^+ + \pi^-)$ (left panel) and $(\Xi^{*0}+\overline{\Xi}^{*0})/(\pi^+ + \pi^-)$ (right panel) measured in pp [8, 37], d–Au [38] and p–Pb as a function of average charged particle density measured at mid-rapidity. Yields of pions for p–Pb collisions are from [14]. Statistical uncertainties (bars) are shown together with total systematic uncertainties (hollow boxes) and systematic uncertainties uncorrelated across multiplicity (shaded boxes). Some model predictions are also shown [24–27] as lines at their appropriate abscissa, respectively.

In Fig. 4 the yields of K, K^{*0}, Λ, Ξ^-, Ω^- relative to the pion yield obtained in pp, p–Pb and Pb–Pb collisions are reported as a function of $\langle dN_{ch}/d\eta\rangle$ measured at mid-rapidity. In pp collisions [17] strange to non-strange integrated particle ratios increase with multiplicity, showing significant enhancement of strange and multi-strange particle production and following the same trend observed in p–Pb collisions despite differences in the initial state and reaching values similar to those observed in Pb–Pb collisions. It is worth noting that the K^{*0}/π ratio in pp collisions at $\sqrt{s}$ = 7 TeV shows hint of the presence of a decreasing trend with multiplicity although not significant given the present uncertainties (Fig. 4). In Fig. 5 the pp and p–Pb hadron-to-pion ratios normalised by the multiplicity-integrated ratio in pp, corresponding to the INEL>0 event class, are reported as a function of multiplicity. While the p/π ratio is practically constant, the increase of strange and multi-strange particles follows a clear hierarchy with strangeness content. Monte Carlo models commonly used for pp collisions at LHC are not able to describe satisfactorily the behaviour of strange and multi-strange particles (see for example Fig. 2 in [17]). While PYTHIA8 [24] doesn't reproduce the observed enhancement with multiplicity in pp collisions, DIPSY [35] and EPOS LHC [36] predict a rising trend with multiplicity, but fail to reproduce the rise correctly. Moreover the predicted proton-to-pion ratio is multiplicity-dependent contrary to the measured one (see Fig. 4)

In Fig. 6 the integrated particle ratios of excited hyperon to pion as $(\Sigma^{*\pm}+\overline{\Sigma}^{*\mp})/2(\pi^+ + \pi^-)$ (left panel) and $(\Xi^{*0}+\overline{\Xi}^{*0})/(\pi^+ + \pi^-)$ (right panel) measured in pp at $\sqrt{s}$ = 7 TeV and p–Pb at $\sqrt{s_{NN}}$ = 5.02 TeV collisions are reported as a function of the average charged particle density and compared to results obtained from STAR in pp and d–Au collisions at $\sqrt{s_{NN}}$ = 200 GeV. An increase of the relative strangeness production with the multiplicity similar to the one observed for the ratio of hyperon to pion (as Λ/π and Ξ^-/π) is observed. The ratios increase gradually and approach thermal model values [26, 27] in the highest multiplicity event class. The constant behaviour of the $\Sigma^{*\pm}/\Lambda$ and Ξ^{*0}/Ξ^- ratios indicates that the observed strangeness enhancement depends predominantly on the hyperon strangeness content rather than on their mass. QCD-inspired predictions clearly underestimate the observed $\Sigma^{*\pm}/\Lambda$ ratios for both pp [24] and p–Pb [25] collisions.

5 Conclusions

In this paper the latest results obtained from ALICE on hadronic resonances have been presented. In particular results on $K^*(892)^0$ and $\phi(1020)$ in pp, p–Pb and Pb–Pb collisions at the various energies studied at LHC both in inclusive and in different multiplicity or centrality intervals, on the $\rho(770)^0$ measured in pp and Pb–Pb collisions at $\sqrt{s_{NN}}$ = 2.76 TeV and on the $\Sigma(1385)^{\pm}$ and $\Xi(1530)^0$ measured in pp collisions at $\sqrt{s}$ = 7 TeV and in p–Pb collisions at $\sqrt{s_{NN}}$ = 5.02 TeV have been shown.

The ALICE Collaboration has measured a centrality-dependent suppression of ρ^0/π and K^{*0}/K ratios in Pb–Pb collisions, which can be described by EPOS calculations with UrQMD to describe hadronic interactions in the hadronic phase [2]. A multiplicity-dependent suppression of the K^{*0}/K ratio is also observed in pp and p–Pb collisions. In contrast, the ϕ/K ratio does not exhibit a centrality- or multiplicity-dependent suppression. This behaviour may be due to the loss of the K^{*0} and ρ^0 signal caused by re-scattering of decay products in the hadronic phase, while the ϕ yield is not affected because of its long lifetime as it decays mostly after the hadronic phase.

From the K^{*0}/K ratio in central Pb–Pb collisions it is possible to estimate a lower limit of hadronic phase lifetime (τ >2 fm/c) [6] using a thermodynamical model [1] which takes into account only the loss of resonances due to re-scattering effects in the hadronic medium. An hadronic lifetime of about 9 fm/c for most central Pb–Pb collisions

is estimated by EPOS followed by a hadronic afterburner phase modeled via UrQMD [2].

The $\Sigma^{*\pm}/\Lambda$ and Ξ^{*0}/Ξ^{-} ratios are not observed to depend on system size or activity in pp and p–Pb collisions, which could mean that the effects of re-scattering and regeneration are not so important for the charged particle densities reached in these colliding systems.

The results in high multiplicity pp collisions have revealed interesting features that are similar to those observed in p–Pb and Pb–Pb collisions. While these features are usually interpreted in Pb–Pb collisions as due to collectivity, their origin in smaller systems is still to be fully understood. An enhanced production of strange and multi-strange particles in high-multiplicity pp collisions with respect to inelastic events has been observed. The magnitude of this strangeness enhancement increases with the event activity, quantified by $\langle \mathrm{d}N_{\mathrm{ch}}/\mathrm{d}\eta \rangle$, and with hadron strangeness. No enhancement is observed for particles with no strange quark content, demonstrating that the observed effect is strangeness rather than mass related. The multiplicity dependence of strangeness production is strikingly similar in pp and p–Pb, and approaches values similar to those obtained in Pb–Pb collisions. None of the current MC models are successful at fully describing these observations, suggesting that further developments are needed for a complete microscopic understanding of strangeness production and indicating the presence of a phenomenon novel in high-multiplicity pp collisions.

References

[1] G. Torrieri and J. Rafelski, J. Phys. G **28**, 1911 (2002); C. Markert *et al.*, aXiv:hep:ph/0206260v2 (2002)
[2] A. G. Knospe *et al.*, Phys. Rev. C **93**, 014911 (2016)
[3] K. Aamodt *et al.* (ALICE Coll.), J. Instrum. **3**, S08002 (2008)
[4] B. Abelev *et al.* (ALICE Coll.), Eur. Phys. J. C **71**, 1594 (2011)
[5] B. Abelev *et al.* (ALICE Coll.), Eur. Phys, J. C **72**, 2183 (2012)
[6] B. Abelev *et al.* (ALICE Coll.), Phys. Rev. C **91**,024609 (2015)
[7] J. Adam *et al.* (ALICE Coll.), Eur. Phys. J. C **76**, 245 (2016)
[8] B. Abelev *et al.* (ALICE Coll.), Eur. Phys. J. C **75**, 1 (2015)
[9] B. Abelev *et al.* (ALICE Coll.), Phys. Rev. Lett. **110**, 032301 (2013)
[10] F. Gelis *et al.*, Annu. Rev. Nucl. Part. Sci. **60**, 463 (2010)
[11] B. Abelev *et al.* (ALICE Coll.), Phys. Lett. B **719**, 29 (2013); B. Abelev *et al.* (ALICE Coll.), Phys. Lett. B **726**, 164 (2013)
[12] G. Aad *et al.* (ATLAS Coll.), Phys. Rev. Lett. **110**, 182302 (2013); G. Aad *et al.* (ATLAS Coll.), Phys. Lett. B **725**, 60 (2013)
[13] V. Khachatryan *et al.* (CMS Coll.), JHEP **09**, 091 (2010); S. Chatrchyan *et al.* (CMS Coll.), Phys. Lett. B **718**, 795 (2013); V. Khachatryan *et al.* (CMS Coll.), Phys. Lett. B **765**, 193 (2017)
[14] B. Abelev *et al.* (ALICE Coll.), Phys. Lett. B **728**, 25 (2014)
[15] J. Adam *et al.* (ALICE Coll.), Phys. Lett. B **758** (2016) 389
[16] V. Khachatryan *et al.* (CMS Coll.), arXiv:1605.06699
[17] J. Adam *et al.* (ALICE Coll.), arXiv:1606.07424 (2016)
[18] B. Abelev *et al.* (ALICE Coll.), Int. J. Mod. Phys. A **29**, 1430044 (2014)
[19] A. Beddall *et al.*, Acta Phys. Polon. B **39**, 173 (2008)
[20] C. Tsallis, J. Stat. Phys. **52**, 479 (1988)
[21] E. Schnedermann *et al.*, Phys. Rev. C **48**, 2462 (1993)
[22] S. A. Bass *et al.*, Prog. Part. Nucl. Phys. **41**, 255 (1998); M. Bleicher *et al.*, J. Phys. G **25**, 1859 (1999)
[23] J. Stachel *et al.*, J. Phys. Conf. Ser. **509**, 012019 (2014)
[24] T. Sjostrand *et al.*, Comput. Phys. Commun. **178**, 852 (2008)
[25] S. Roesler *et al.*, *Conference Proceedings MC2000* (Lisbon, Portugal, October 23-26, 2000) 1033–1038, hep-ph/0012252
[26] A. Andronic *et al.*, Phys. Lett. B **673**, 1420145 (2009)
[27] S. Wheaton *et al.*, Comp. Phys. Commun. **180**, 84 (2009)
[28] J. Rafelski *et al.*, Phys. Rev. Lett. **48**, 1066 (1982); P. Koch *et al.*, Phys. Rep. **142**, 167 (1986)
[29] E. Andersen *et al.*, Phys. Lett. B **433**, 209 (1998); E. Andersen *et al.* (WA97 Coll.), Phys. Lett. B **449**, 401 (1999)
[30] S. V. Afanasiev *et al.* (NA49 Coll.), Phys. Lett. B **538**, 275 (2002); T. Anticic *et al.* (NA49 Coll.), Phys. Rev. Lett. **93**, 022302 (2004)
[31] F. Antinori *et al.* (NA57 Coll.), Phys. Lett. B **595**, 68 (2004); F. Antinori *et al.* (NA57 Coll.), J. Phys. G **37**, 045105 (2010)
[32] J. Adams *et al.* (STAR Coll.), Phys. Rev. Lett. **92**, 182301 (2004); J. Adams *et al.* (STAR Coll.), Phys. Rev. Lett. **98**, 062301 (2007); B. I. Abelev *et al.* (STAR Coll.), Phys. Rev. C **77**, 044908 (2008)
[33] B. Abelev *et al.* (ALICE Coll.), Phys. Lett. B **728**, 216 (2014) [Erratum: Phys. Lett. B **734**, 409 (2014)]
[34] B. Abelev *et al.* (ALICE Coll.), Phys. Rev. Lett. **111**, 222301 (2013)
[35] C. Bierlich *et al.*, JHEP **03**, 148 (2015)
[36] T. Pierog *et al.*, Phys. Rev. C **92**, 034906 (2015)
[37] J. Adam *et al.* (ALICE Coll.), Eur. Phys. J. C **75**, 226 (2015)
[38] B. I. Abelev *et al.* (STAR Coll.), Phys. Rev. C **78**, 044906 (2008)